JCB Article

p107 regulates neural precursor cells in the mammalian brain

Jacqueline L. Vanderluit,[1] Kerry L. Ferguson,[1] Vassiliki Nikoletopoulou,[1] Maura Parker,[3] Vladimir Ruzhynsky,[1] Tania Alexson,[2] Stephen M. McNamara,[1] David S. Park,[1] Michael Rudnicki,[3] and Ruth S. Slack[1]

[1]Neuroscience Research Group, Ottawa Health Research Institute, Ottawa, Ontario, Canada K1H 8M5
[2]Neurobiology Research Group, Department of Anatomy and Cell Biology, University of Toronto, Toronto, Ontario, Canada M5S 1A8
[3]Molecular Medicine Program, Ottawa Health Research Institute, Ottawa, Ontario, Canada, K1H 8L6

Here we show a novel function for Retinoblastoma family member, p107 in controlling stem cell expansion in the mammalian brain. Adult p107-null mice had elevated numbers of proliferating progenitor cells in their lateral ventricles. In vitro neurosphere assays revealed striking increases in the number of neurosphere forming cells from $p107^{-/-}$ brains that exhibited enhanced capacity for self-renewal. An expanded stem cell population in p107-deficient mice was shown in vivo by (a) increased numbers of slowly cycling cells in the lateral ventricles; and (b) accelerated rates of neural precursor repopulation after progenitor ablation. Notch1 was up-regulated in $p107^{-/-}$ neurospheres in vitro and brains in vivo. Chromatin immunoprecipitation and p107 overexpression suggest that p107 may modulate the Notch1 pathway. These results demonstrate a novel function for p107 that is distinct from Rb, which is to negatively regulate the number of neural stem cells in the developing and adult brain.

Introduction

The discovery of stem cells in the adult mammalian brain has generated great potential for therapeutic strategies to facilitate brain regeneration after injury (Reynolds and Weiss, 1992). Currently, the use of stem cells as a therapeutic tool is confounded by our lack of knowledge in the regulation and expansion of the stem cell pool. To expand or maintain the stem cell pool, stem cells can undergo self-renewing cell divisions whereby one or both daughter cells are stem cells (Morrison et al., 1997). Stem cells also undergo differentiative divisions, where one or both daughter cells are progenitor cells, having the potential to differentiate into neurons, astrocytes, or oligodendrocytes (Reynolds and Weiss, 1992; Morrison et al., 1997). Although recent studies have demonstrated that the Notch-signaling pathway is necessary for self-renewing stem cell divisions (Nakamura et al., 2000; Ohtsuka et al., 2001; Hitoshi et al., 2002), the mechanism regulating whether the cell undergoes a self-renewing versus differentiative division is poorly understood, particularly in the adult brain.

Cell cycle genes have been found to play an important role in brain development. For example, the retinoblastoma tumor suppressor protein (Rb) has been shown to regulate the terminal mitosis of committed neuroblasts, such that embryos lacking pRb exhibit enhanced neuroblast proliferation, ectopic cell division, and enlarged brains (Clarke et al., 1992; Jacks et al., 1992; Lee et al., 1992; Ferguson et al., 2002; MacPherson et al., 2003; Wu et al., 2003). The Rb family consists of three closely related proteins, pRb, p107, and p130, characterized by a pocket domain that interacts with proteins such as the E2F family of transcription factors (Ferguson and Slack, 2001; Stevaux and Dyson, 2002). Considerable evidence suggests that Rb family proteins have overlapping functions, which is best exemplified by studies examining mice with targeted Rb mutations (Clarke et al., 1992; Jacks et al., 1992; Lee et al., 1992; Lee et al., 1994). Whereas Rb deficiency results in embryonic lethality (Clarke et al., 1992; Jacks et al., 1992; Lee et al., 1992) mice deficient in either p107 or p130 develop normally on a C57BL/6 genetic background (Cobrinik et al., 1996; Lee et al., 1996). In contrast, when p107- or p130-null mice are interbred with mice carrying a null mutation for Rb, the phenotype is

Address correspondence to Dr. Ruth S. Slack, Neuroscience Research Group, Ottawa Health Research Institute, 451 Smyth Rd., Ottawa, ON, K1H 8M5. Tel.: (613) 562-5800, ext. 8458. Fax: (613) 562-5403. email: rslack@uottawa.ca

Key words: neural stem cells, self-renewing division, regeneration

Abbreviations used in this paper: CNS, central nervous system; Rb, retinoblastoma.

exacerbated, indicating that p107/p130 can partially substitute for pRb (Lee et al., 1996; Lipinski and Jacks, 1999). Biochemical studies suggest that Rb family members have distinct binding preferences and exhibit tissue specific expression patterns (Ewen et al., 1992; Faha et al., 1992; Lees et al., 1992; Li et al., 1993; Lipinski and Jacks, 1999; Stevaux and Dyson, 2002). In the developing brain, pRb is expressed in both dividing precursor cells and in postmitotic neurons. In contrast, the expression of p107 is restricted to the ventricular zone, and becomes rapidly downregulated at the onset of differentiation (Gill et al., 1998; Callaghan et al., 1999; Ferguson and Slack, 2001), whereas p130 exhibits highest expression in postmitotic neurons (Jiang et al., 1997; Yoshikawa, 2000). Although p107 has distinct binding preferences and tissue-specific distribution, no biological role, which is unique from Rb, has been identified.

Because p107 is highly expressed in the germinal zone with a pattern distinct from Rb, the goal of this study was to determine whether p107 may play a unique role in neural precursor cell regulation. In the present study, we report that p107 has a distinct role from pRb, specifically in regulating the neural precursor population with stem cell characteristics.

Results

p107 is highly expressed in cells of the embryonic ventricular zone and of the subependyma in adult mice

At the present time, little is known regarding the genes that regulate the neural stem cell population or the transition from stem cell to progenitor cell. Unlike other Rb family proteins, the expression of p107 is restricted to the neural precursor cells in the ventricular zone (Jiang et al., 1997). Due to its unique expression pattern, we asked whether p107 was also expressed in the neural precursor population in adults. In situ hybridization revealed p107 mRNA expression in a few select cells along the lateral ventricles of adult wild-type mice (Fig. 1 a). In vitro examination of p107 protein expression by Western analysis showed that p107 is expressed in neural precursor cells from wild-type embryonic day 10 and adult neurospheres (Fig. 1 d). Because p107 expression is maintained in the adult neural precursor population, we questioned whether it may have a specific role in precursor cell regulation.

p107$^{-/-}$ mice exhibit increased levels of neural precursor cells

To ask whether p107 regulates the neural precursor population in vivo, we first determined if the absence of p107 affected the number of progenitor cells in the adult brain. The cell cycle time of neural progenitor cells in the adult brain has been estimated to be 12.7 h (Morshead and van der Kooy, 1992). Therefore, to assess the number of constitutively proliferating progenitor cells in adult brains, a series of BrdU injections was given over 10.5 h. Adult p107$^{-/-}$ brains had 50% more constitutively proliferating cells (32,044 ± 2,605 cells) than littermate controls (21,480 ± 1,902 cells) as determined by BrdU labeling (Fig. 2, a–c). Based on these results, we questioned whether p107 might affect the expression of genes involved in the regulation of the neural precursor population.

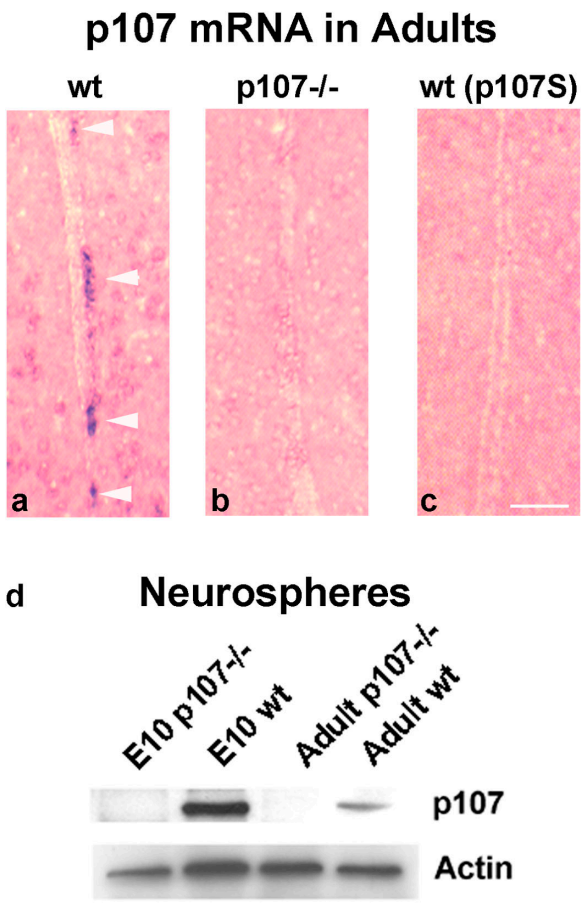

Figure 1. **p107 is expressed in neural precursor cells.** In situ hybridization with an antisense riboprobe for p107 revealed (a) p107 mRNA expression only within a small population of cells in the lateral ventricles of wild-type mouse brains, and (b) the absence of p107 mRNA expression in brains from p107$^{-/-}$ mice. (c) A p107 sense riboprobe was used as a control on wild-type mouse brains. (d) Western blot analysis revealed high levels of p107 expression in neural precursor cells from embryonic day 10 and adult wild-type neurospheres. p107-S, p107 sense probe. Bar, 50 μm.

Enhanced Notch signaling in p107$^{-/-}$ mice

The Notch signaling pathway has been previously shown to regulate the neural stem cell pool (Hitoshi et al., 2002). To determine whether Notch signaling was affected in p107$^{-/-}$ neural precursor cells, we first examined expression of members of the Notch-signaling pathway including Notch1, Delta-like1, Hes1, and Hes5. In situ hybridization revealed that p107-deficient embryo brains expressed strikingly higher levels of Notch1 (Fig. 3, a and b) as well as its ligand, Delta-like1 (Fig. 3, c and d) and downstream target Hes1 (Fig. 3, e and f). In contrast, no difference was observed in the level of the Hes5 mRNA signal, also a downstream target of Notch (Fig. 3, g and h). To determine whether there was increased Notch activation, activated Notch was assessed by Western analysis using an antibody directed against the cleaved intracellular fragment (Robey et al., 1996). Consistent with higher levels of Notch1 ex-

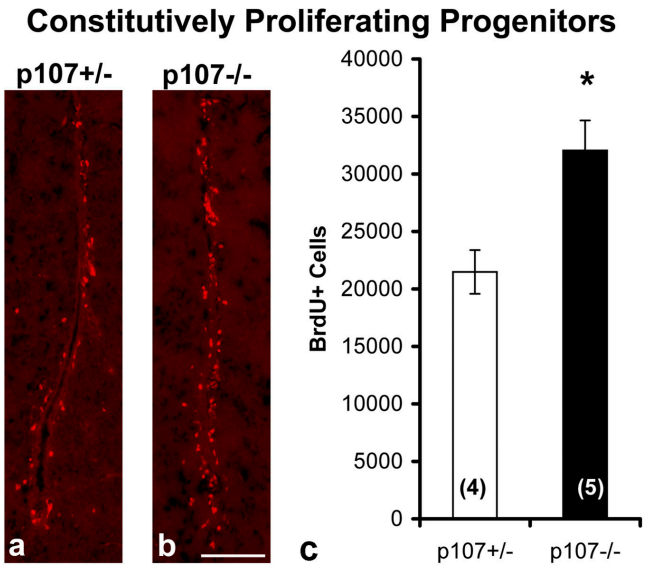

Figure 2. **Enhanced progenitor cell numbers in adult p107-null mice.** Short-term (10.5 h) BrdU application revealed a 1.5-fold increase in the number of constitutively proliferating progenitor cells in adult $p107^{-/-}$ mice versus $p107^{+/-}$ (a–c). Bar, 200 μm. Significance at $^*P < 0.01$.

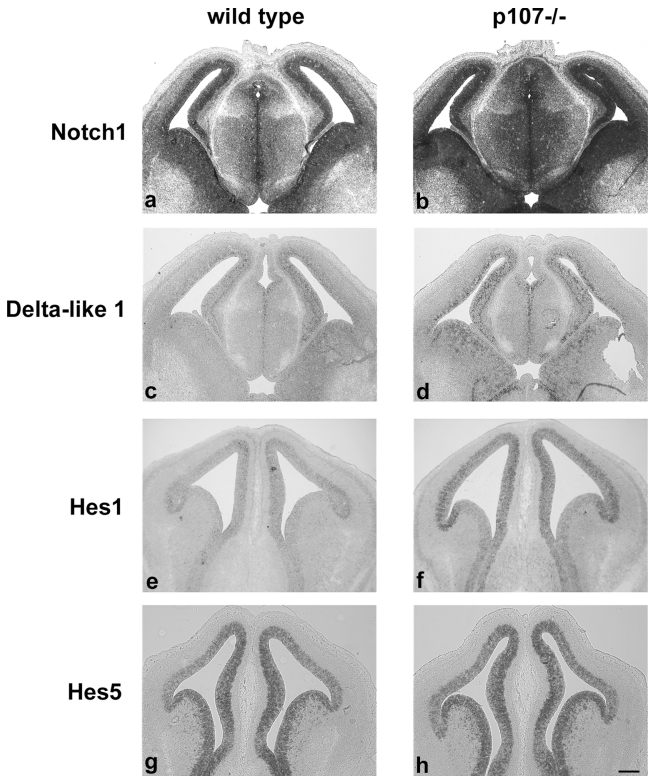

Figure 3. **Enhanced expression of members of the Notch signaling pathway.** Higher levels of Notch1 mRNA and its signaling components, Delta-like 1 and Hes1, in $p107^{-/-}$ mice than its wild-type littermates. In situ hybridization was performed on embryonic day 14 $p107^{-/-}$ and wild-type littermates using riboprobes for Notch1 (a and b), Delta-like1 (c and d), Hes1 (e and f), and Hes5 (g and h). Note higher in situ hybridization signals for Notch1, Delta-like1, and Hes1 were consistently observed in $p107^{-/-}$ mice versus their wild-type littermates ($n = 3$ per genotype). Bar, 200 μm.

pression, $p107^{-/-}$ precursor cells exhibited a clear enhancement of both full-length (260 kD) and activated Notch1 (120 kD; Fig. 4 a).

Because p107 has been shown to interact primarily with E2F transcription factors, we examined the Notch1 gene for E2F consensus sequences. Putative E2F binding sites were detected in the first two introns and 3′ sequences of the mouse Notch1 gene. To determine whether p107 may regulate Notch1, chromatin immunoprecipitations were per-

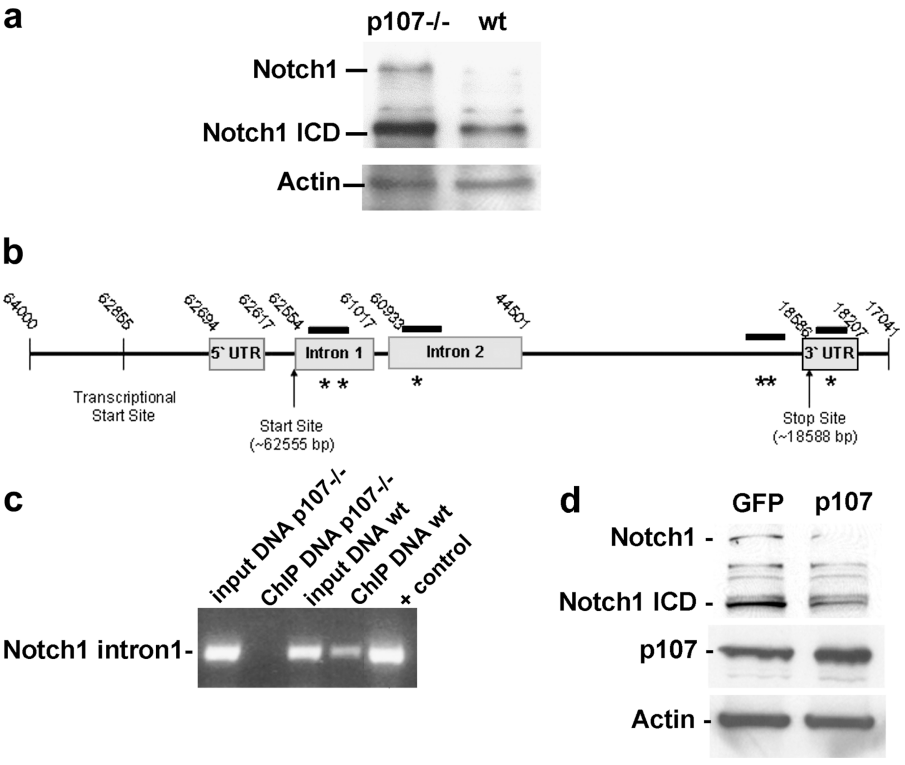

Figure 4. **Higher levels of activated Notch1 in $p107^{-/-}$ neurospheres.** (a) Western analysis of protein lysates from E10 neurospheres revealed $p107^{-/-}$ neurospheres had higher levels of both full-length Notch1 (~260 kD) and the activated intracellular domain of Notch1 (160 kD). (b) Examination of the Notch1 gene revealed E2F binding sequences within the first two introns and 3′ region where p107 might potentially interact. (c) Chromatin immunoprecipitation of adult neurospheres and E14 telencephalic neuroepithelia using a p107 antibody showed interaction of p107 with E2F sites in the first intron of the Notch1 gene ($n = 3$). (d) Overexpression of p107 in HEK 293 cells down-regulated expression of Notch1 protein (full length) and Notch1 activity.

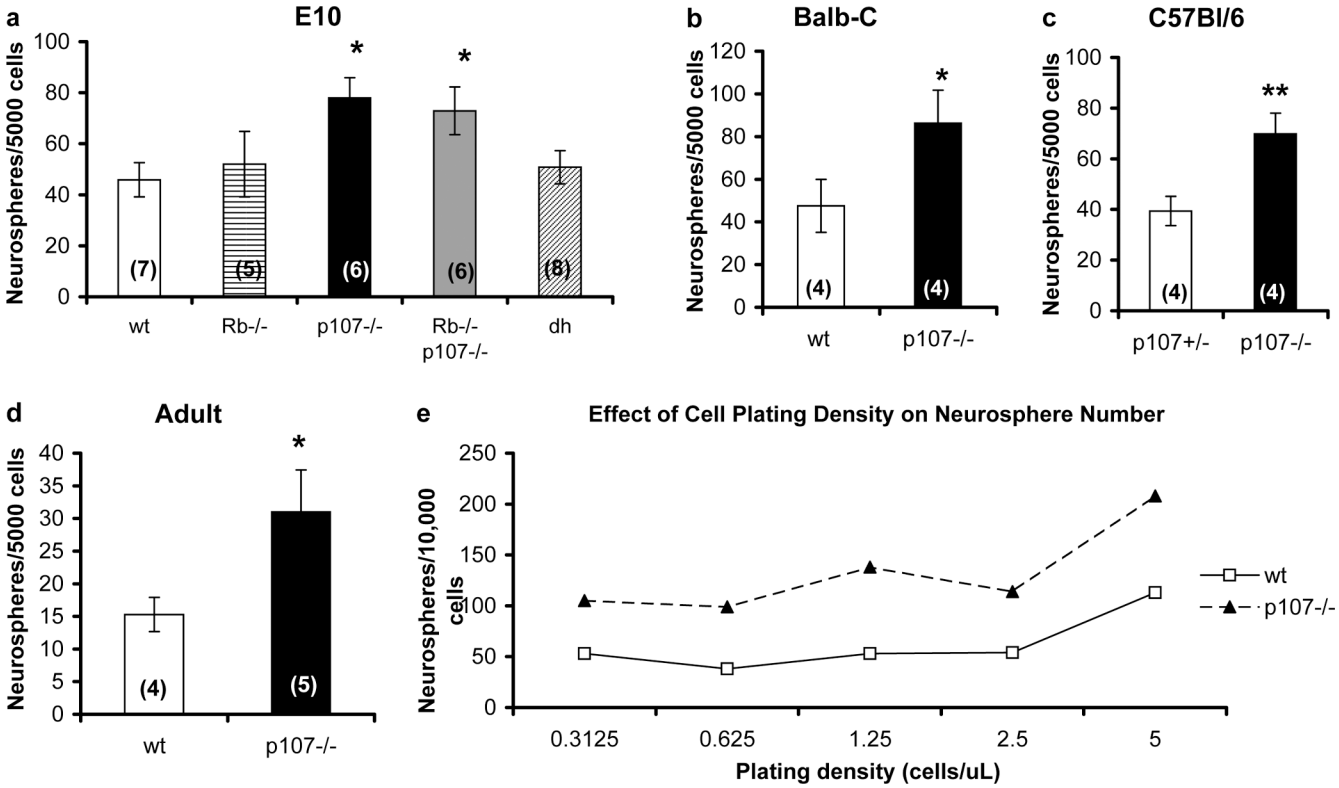

Figure 5. **Increased numbers of neurosphere-forming cells in p107$^{-/-}$ embryos and adult mice.** (a) The telencephalic neuroepithelia of day 10 embryos from p107$^{-/-}$ and Rb$^{-/-}$:p107$^{-/-}$ generated significantly more neurospheres than wild-type and heterozygote controls. E10 p107$^{-/-}$ mice on (b) pure Balb-C or (c) pure C57Bl/6 backgrounds also generated more primary neurospheres than controls indicating that p107 affects the number of neurosphere forming cells independent of mouse strain. (d) The ventricular subependyma of adult p107$^{-/-}$ mice generated significantly more primary neurospheres than wild-type controls. (e) E10 wild-type and p107$^{-/-}$ neural precursors cells were plated across a dilution series from high to low concentrations such that at each concentration 10,000 cells were plated. After 7 d, counts of the total number of neurospheres formed per dilution revealed p107$^{-/-}$ cultures consistently produced more neurospheres than wild-type cultures. Note plating density only affected neurosphere number at the highest cell density 5 cells/μl^{-1}. Significance at *P $<$ 0.05 and **P $<$ 0.01.

formed using a p107 antibody on fixed chromatin from neurosphere cultures. Using four sets of PCR primers for E2F sites in (a) intron 1, (b) intron 2, and (c and d) two E2F sites in the 3′ regulatory region. We found p107 binding to E2F sites in intron 1 of the Notch1 gene (Fig. 4, b and c). These results demonstrate that p107 binds to Notch1 regulatory sequences on native chromatin, suggesting an interaction between p107 and the Notch1 pathway.

To assess whether p107 directly regulates Notch1 expression, we used recombinant adenoviral vectors to express p107 protein in Notch1-expressing HEK 293 cells. Enhanced expression of p107 resulted in down-regulation of Notch1 protein and activity (Fig. 4 d). These data support the interpretation that p107 affects stem cell self-renewal by regulating self-renewing divisions through interactions with the Notch1-signaling pathway.

p107 regulates the number of neurosphere-forming cells

Considering p107$^{-/-}$ mice have enhanced Notch activity and Notch has been previously shown to regulate stem cell numbers, we asked whether the increased progenitor population in p107$^{-/-}$ mice may result from an expansion in the size of the neural stem cell pool. To estimate the size of the neural stem pool at different stages of development, we used the in vitro neurosphere assay (Reynolds and Weiss, 1992), which identifies stem cells according to their (a) multipotentiality and (b) self-renewal capacity (Potten and Loeffler, 1990). Each neurosphere that exhibits these characteristics is believed to arise from a single neural stem cell (Reynolds and Weiss, 1992). Embryonic day 10 mice with the following genotypes: Rb$^{-/-}$, p107$^{-/-}$, Rb/p107 compound-null (Rb$^{-/-}$:p107$^{-/-}$), double heterozygotes (Rb$^{+/-}$:p107$^{+/-}$), and wild-type littermates, were assayed for neurosphere-forming cells. Cultures from p107$^{-/-}$ and Rb$^{-/-}$:p107$^{-/-}$ embryonic telencephalic neuroepithelia generated significantly greater numbers of primary neurospheres relative to control littermates (Fig. 5 a). In contrast, the number of neurospheres in Rb$^{-/-}$ cultures was not significantly different from wild-type or double heterozygote cultures. This experiment was reproduced with inbred Balb-C and C57Bl/6 mice (Fig. 5, b and c) to confirm that this was not due to strain effects. Our results show therefore, that p107 regulates the number of neurosphere-forming cells in the embryonic brain, a function that is distinct from Rb.

Because stem cell properties and frequency differ as development proceeds, we asked whether p107 may regulate the number of neurosphere-forming cells in adult brains. Adult p107$^{-/-}$ cultures exhibited a dramatic effect resulting in a twofold increase in the number of primary neurospheres generated (Fig. 5 d). Taken together, these results demon-

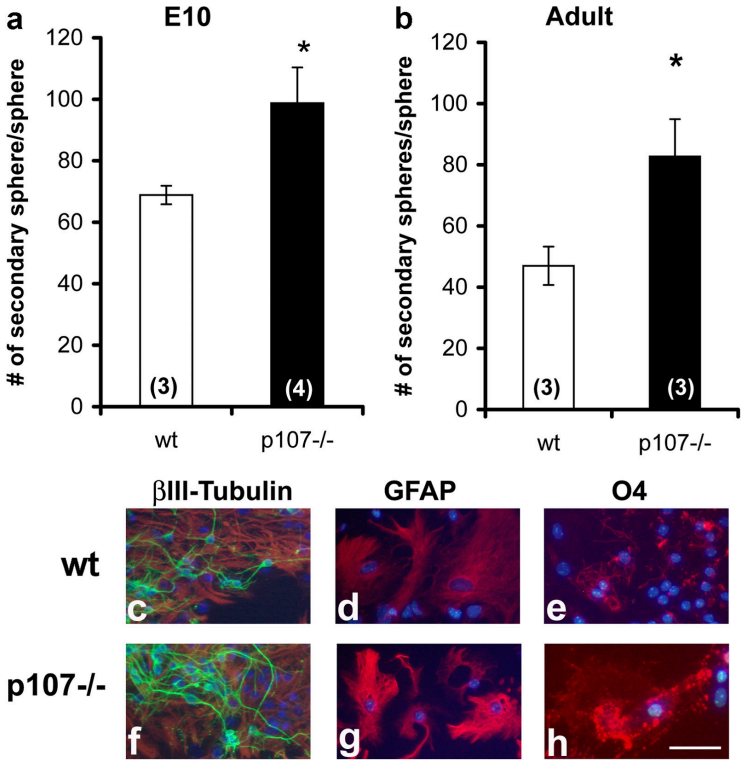

Figure 6. **p107$^{-/-}$ and wild-type neurospheres possess properties consistent with neural stem cells.** (a) E10 and (b) adult p107$^{-/-}$ neural stem cells show a higher rate of self-renewal than wild-type littermates when cultured in the presence of bFGF alone. Neurospheres from wild-type (c–e) and p107-null (f–h) mice are multipotent and differentiate into: (c and f) neurons (βIII-tubulin, green), (d and g) astrocytes (GFAP, red), and (e and h) oligodendrocytes (O4, red). Bar, 50 μm. Significance at *$P < 0.05$.

strate that p107 controls the number of neurosphere-forming cells in the developing and adult brain.

To assess whether the effect of p107 on the number of neurosphere-forming cells was cell autonomous or non-cell autonomous, cells were plated along a dilution curve. 10,000 cells were plated at each cell density and 1 wk after plating the total number of neurospheres formed at each cell density was counted. If the total number of neurospheres changed with increasing cell density one would interpret a non-cell autonomous effect, whereas if the total number of neurospheres formed was similar across the dilution range one would expect a cell autonomous effect. Our results show that independent of cell density, p107$^{-/-}$ cultures consistently produced more neurospheres than wild-type cultures (Fig. 5 e). Initial plating densities ranging from 0.3125 to 2.5 cells/μl^{-1} resulted in a mean of 114 neurospheres/10,000 cells in cultures from p107$^{-/-}$ neural precursors versus 50 neurospheres/10,000 cells in cultures from wild-type neural precursors. Considering that across the four lowest dilutions there was no difference in the total number of neurospheres formed in p107$^{-/-}$ cultures, the effect of p107 on the number of neurosphere-forming cells appears to be cell autonomous.

Neurospheres are derived from stem cells

Whereas neurospheres may arise from progenitor cells as well as stem cells, progenitor-derived neurospheres fail to self-renew (Chiasson et al., 1999). Two characteristics that distinguish a neural stem cell from a progenitor cell are: (a) self-renewal capacity; and (b) multipotentiality. Consistent with a role in stem cell regulation, p107-deficient neurospheres exhibited an enhanced self-renewal capacity. Specifically, embryonic p107$^{-/-}$ primary neurospheres produced 99 ± 12 secondary neurospheres in contrast to 68 ± 3 by wild-type neurospheres (Fig. 6 a). This was even more striking in the adult, where a twofold increase was observed with p107$^{-/-}$ neurospheres producing 83 ± 12 secondary neurospheres in contrast to 47 ± 6 generated by wild-type neurospheres (Fig. 6 b). Thus, adult and embryonic p107$^{-/-}$ neurospheres produced significantly more secondary neurospheres, consistent with enhanced self-renewing cell divisions.

Multipotentiality was assessed after differentiation of neurospheres by immunohistochemistry with antibodies to identify neurons (βIII-tubulin), astrocytes (glial fibrillary acidic protein), and oligodendrocytes (O_4 antigen; Fig. 6, c–h). Individual differentiated neurospheres from wild-type (Fig. 6, c–e) and p107-null brains (Fig. 6, f–h) at embryonic (Fig. 6, c–h) and adult ages (unpublished data) generated all three cell types, indicating that these neurospheres arose from a multipotent cell. These results, in combination with the demonstrated self-renewal capacity suggest that neurospheres in both p107$^{-/-}$ and wild-type cultures originate from stem cells.

p107 regulates neural stem cells in vivo

Studies have shown that, in vivo, adult neural stem cells are relatively quiescent and cycle very slowly at ~15 d, in contrast to constitutively proliferating cells that have a cell cycle time of 12.7 h (Morshead and van der Kooy, 1992; Reynolds and Weiss, 1992; Morshead et al., 1994, 1998). To assess the neural stem cell pool in vivo, we used two approaches that exploited their slow cell cycle kinetics: (a) BrdU labeling of slowly dividing cells; and (b) assaying the regenerative response after [^{3}H]thymidine progenitor ablation.

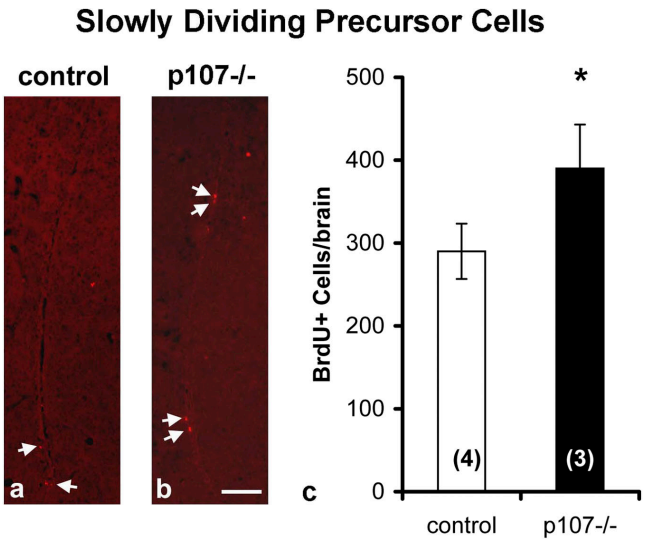

Figure 7. **p107-deficient mice have higher numbers of slowly dividing neural precursor cells in the adult brain.** (a–c) Long-term BrdU labeling revealed a significantly larger population of slowly dividing cells in adult p107-null mice than controls. 4 wk after BrdU injections, the slowly dividing cells in the ventricular subependyma of adult control and $p107^{-/-}$ mice retain their BrdU label. Bar: (a and b) 100 μm. Significance at $^*P < 0.05$.

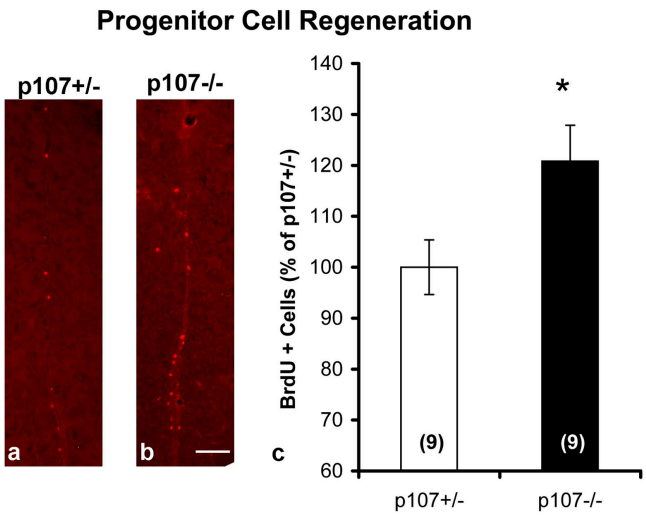

Figure 8. **Enhanced regeneration of constitutively proliferating progenitors in p107-null mice.** After a [^{3}H]thymidine kill of the proliferating progenitors, significantly greater numbers of BrdU-labeled cells were found along the lateral ventricle subependyma of $p107^{-/-}$ mice versus $p107^{+/-}$ mice indicative of recruitment of a larger number of stem cells in $p107^{-/-}$ mice (a–c). Bar: (a and b) 200 μm. Significance at $^*P < 0.05$.

Slowly dividing cells in the ventricular subependyma of adult brains were labeled with BrdU over 12 h, and examined 4 wk later. After 4 wk, the rapidly cycling progenitor cells will: (a) dilute out the label (cell cycle <24 h); (b) undergo apoptosis; or (c) differentiate and migrate away from the ventricular zone into the cortical plate. Thus, the only cells that retain the label in the ventricular zone are the slowly cycling neural stem cells. This assay has been previously shown to correlate well with the neurosphere assay (Morshead et al., 1998). p107-null brains had significantly more BrdU-positive cells in the ventricular subependyma than littermate controls (Fig. 7, a–c). Thus, based on previous studies, these slowly proliferating cells are considered to represent the stem cell population.

As a second indication of the size of the stem cell population, we asked whether p107-deficient mice exhibited enhanced progenitor regeneration after ablation. Application of high doses of [^{3}H]thymidine kills actively dividing cells but not the slowly cycling stem cells. A 12-h treatment of [^{3}H]thymidine, therefore depletes the rapidly proliferating progenitors whereas the majority of stem cells would be unaffected. To measure the rate of regeneration, cycling cells were labeled with BrdU over a 10.5-h time course to label all proliferating cells in the germinal zones. Consistent with an expanded stem cell pool, p107-deficient mice revealed a significant increase in the rate of progenitor regeneration (Fig. 8, a and b). Quantification of BrdU-labeled cells revealed 120% more BrdU-positive cells in the ventricular subependyma of $p107^{-/-}$ mouse brains (8,918 ± 876) versus $p107^{+/-}$ controls (7,689 ± 973; Fig. 8 c). Thus, in vivo studies measuring (a) slowly proliferating cells and (b) progenitor regeneration are consistent with results obtained from the in vitro neurosphere assay suggesting an expanded neural stem cell pool in the absence of p107.

Does an increase in the size of the progenitor cell population result in enhanced neurogenesis?

Neurogenesis occurs constantly in the adult olfactory system, in which newly committed progenitor cells originating from the subependyma of the lateral ventricles migrate along the rostral migratory stream to the olfactory bulb (Corotto et al., 1993; Luskin, 1993; Lois and Alvarez-Buylla, 1994; Lois et al., 1996). The enhanced numbers of progenitor cells along the ventricle in adult $p107^{-/-}$ mice led us to question whether there may be increased olfactory neurogenesis. Adult mice received intraperitoneal injections of BrdU to label newly born progenitor cells and 4 wk later were killed. New neurons in the olfactory bulb were identified by double labeling with BrdU and the neuronal marker, NeuN (Shingo et al., 2003). The numbers of new neurons and BrdU-positive cells in the olfactory bulb did not differ between $p107^{-/-}$ and wild-type mice (Table I). These results suggest that despite an increase in the neural precursor pool in $p107^{-/-}$ mice, neurogenesis was not increased in the olfactory bulb.

To account for this apparent discrepancy, we assessed whether there was a higher rate of apoptosis in $p107^{-/-}$ mouse brains. TUNEL-positive cells within the ventricular subependyma were counted in every 10th section through the brains of adult wild-type and $p107^{-/-}$ mice. Counts revealed that adult p107-null mice had significantly more

Table I. **Neurogenesis in the olfactory bulb of $p107^{-/-}$ mice**

	BrdU$^+$	BrdU and NeuN$^+$
Control	128 ± 19	58 ± 9
$p107^{-/-}$	135 ± 13	61 ± 6

Counts of periglomerular cells (BrdU) and periglomerular neurons (BrdU and NeuN) in the olfactory bulb 4 wk after BrdU injections.

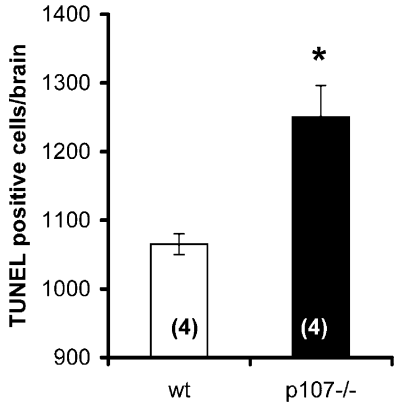

Figure 9. **Increased apoptosis in p107$^{-/-}$ brains.** To determine whether the enhanced numbers of progenitor cells in the ventricle was maintained by apoptosis, TUNEL staining was performed on coronal sections through the lateral ventricles. p107$^{-/-}$ mice had significantly more TUNEL-positive cells throughout the ventricle subependyma than wild-type littermates. Significance at *P $<$ 0.05.

apoptotic cells (1,250 $\pm$ 46) within the ventricular subependyma compared with wild-type controls (1,065 $\pm$ 15; Fig. 9). These findings suggest that the greater numbers of progenitor cells in p107$^{-/-}$ mice and the enhanced numbers of neurospheres in vitro are controlled in vivo by a higher rate of apoptosis. Furthermore, these results show that the larger progenitor cell pool in p107-null brains cannot be attributed to a reduction in progenitor cell death.

In summary, our results with in vitro neurosphere assays together with our in vivo assays strongly support a role for p107 in regulating the number of neural stem cells in the brain. This enhanced rate of stem cell self-renewal is regulated in vivo by increased apoptosis of p107-deficient progenitor cells, which likely functions to maintain homeostasis in the regulation of neurogenesis and brain size.

Discussion

The results of this study demonstrate that p107 plays a role in regulating the expansion of the stem cell population in the embryonic and adult mammalian brain. This is evident in vitro by enhanced numbers of primary neurospheres in p107-null cultures and in vivo by a larger population of slowly dividing precursor cells in adult p107-null mice. This was further supported in vivo by a more rapid regeneration of the progenitor pool after [^{3}H]thymidine ablation of proliferating progenitors. Enhancement of neural stem cell numbers in p107$^{-/-}$ mice is attributed to a greater self-renewal capacity, as demonstrated by secondary neurosphere production as an assay of self-renewing divisions. Increased stem cell self-renewal in the absence of p107 was further supported by deregulation of the Notch signaling molecules and activation of the Notch pathway. These studies demonstrate a novel role for p107 that is distinct from other Rb family members, and may represent a potential therapeutic strategy for stem cell activation.

p107$^{-/-}$ mice have an expanded population of stem cells

Our initial observations revealed that p107-deficient brains exhibit greater numbers of proliferating progenitor cells in the lateral ventricles, which led us to question whether this phenotype could arise from enhanced levels of neural stem cells. As there are no definitive markers of neural stem cells, we used the in vitro neurosphere assay for a quantitative assessment of neural stem cell numbers. Our results showed a significant increase in the number of neurosphere-forming cells from p107$^{-/-}$ mouse brains during development and in adults. Even when neural precursors were plated along a dilution curve, p107$^{-/-}$ cultures consistently produced more neurospheres than wild-type cultures. Importantly, p107$^{-/-}$ cultures produced on average 114 neurospheres/10,000 cells at high plating densities of 2.5 cells/μl^{-1} and at the lowest plating density of 0.3125 cells/μl^{-1}. This suggests that the effect of p107 on the number of neurosphere-forming cells is due to a cell autonomous mechanism.

Recently, limitations of the neurosphere assay have shown that neurospheres can arise from progenitor cells as well as stem cells, however progenitor-derived neurospheres fail to self-renew (Chiasson et al., 1999). This issue was addressed by the demonstration of the self-renewal capacity and multipotentiality of both wild-type and p107$^{-/-}$ neurospheres. Due to a lack of markers to specifically identify neural stem cells, we used two in vivo assays that can distinguish stem cells from progenitors by exploiting their slow cell cycle kinetics. First, long-term BrdU labeling revealed significantly greater numbers of slowly cycling stem cells in adult p107$^{-/-}$ brains. Consistent with this, a second assay was used whereby p107-deficient brains exhibited an enhanced rate of progenitor repopulation after [^{3}H]thymidine ablation. In these experiments, the loss of progenitors resulted in the recruitment of stem cells into the cell cycle to repopulate the damaged ventricular zone. Consistent with an expanded stem cell pool, p107-deficient adult brains revealed an enhanced rate of progenitor repopulation. Taken together, our quantitative in vitro neurosphere assay and in vivo findings demonstrate that p107-deficient brains contain expanded stem cell pools that persist into adulthood.

p107 controls self-renewing stem cell divisions

p107 may regulate neural stem cell number in the brain by regulating the type of cell division. The formation of secondary neurospheres from a single primary neurosphere is indicative of a self-renewing stem cell division (Reynolds and Weiss, 1996). Higher numbers of secondary neurospheres generated, indicate that p107-deficient neural stem cells underwent a higher proportion of self-renewing or symmetric cell divisions leading to an expansion of the stem cell pool. As p107 appears to have a cell autonomous effect on self-renewing stem cell division, we examined whether there were differences between p107$^{-/-}$ brains and wild-type brains with regards to the Notch signaling pathway. Previous studies have shown that Notch signaling enhances stem cell self-renewal and thereby maintains cells in a proliferative mode (Chen et al., 1997; Hitoshi et al., 2002). This is best exemplified in the brains of Notch1 and Hes1-null mice, which exhibit depleted stem cell numbers with reduced self-

renewing capacity (Nakamura et al., 2000; Ohtsuka et al., 2001; Hitoshi et al., 2002). Consistent with more self-renewing cell divisions, $p107^{-/-}$ brains had higher levels of expression of members of the Notch1–Hes signaling pathway together with enhanced Notch1 activity, as demonstrated by higher levels of activated Notch1 intracellular domain and its downstream target, Hes1. Furthermore, chromatin immunoprecipitation demonstrated binding of p107 on E2F consensus sites of Notch1 regulatory sequences, and p107 overexpression resulted in down-regulation of Notch1 protein and activation, both suggesting that Notch1 may be regulated by p107. Taken together these data support a role for p107 in regulating self-renewing neural stem cell division through enhanced Notch1 activity.

The progenitor population is regulated by apoptosis

In the rodent brain, a proportion of the neural progenitors arising in the subventricular zone migrate to the olfactory bulb, where a continual turnover in olfactory neurons takes place (Corotto et al., 1993; Luskin, 1993; Lois and Alvarez-Buylla, 1994; Lois et al., 1996). Despite ongoing progenitor proliferation in the ventricular subependyma of the adult mammalian brain, there is no increase in brain size. One explanation is that the brain cannot support excessive levels of precursor cells due to limiting amounts of growth factors. Thus in the healthy brain, homeostasis is maintained by increasing the rate of apoptosis to compensate for excessive numbers of neural precursor cells. Indeed, recent studies have demonstrated ongoing apoptosis in the adult subventricular zone (Biebl et al., 2000; Levison et al., 2000; Lindsten et al., 2003). The enhanced pool of constitutively proliferating progenitor cells in $p107^{-/-}$ mice and the absence of any changes in olfactory neurogenesis led us to question whether increases in progenitor cell number would be regulated by a corresponding increase in cell death. Our results demonstrate that this occurs in the p107-null brains, in which increased numbers of TUNEL-positive cells in the ventricular subependyma were observed. Since apoptotic cells are only TUNEL positive for ~2 h during the progression of apoptosis, the number of TUNEL-positive cells is likely an underestimate of the total number of cells undergoing cell death at a given time (Rossiter et al., 1996). Hence, these results support the hypothesis that fluxes in the neural progenitor pool in vivo are tightly regulated by corresponding changes in cell death. Therefore, if p107 is to serve as a potential therapeutic target to enhance the stem cell population in vivo, mechanisms to enhance precursor survival would also need to be addressed.

p107 has a unique function, distinct from pRb

Previous studies have suggested that, due to sequence similarity, and the nonlethal phenotype of p107-null mice, the role of p107 overlaps significantly with that of pRb (Lee et al., 1996). Binding assays have demonstrated that Rb family members have distinct individual binding preferences. For example, pRb preferentially binds E2F 1, 2, and 3, whereas p107 and p130 bind E2F 4 and 5 (Beijersbergen et al., 1994; Ginsberg et al., 1994; Hijmans et al., 1995; Vairo et al., 1995). In addition, both p107 and p130, but not pRb, interact with cyclinE/cdk2 and cyclinA/cdk2 (Ewen et al., 1992; Faha et al., 1992; Lees et al., 1992; Li et al., 1993). Although p107 has been shown to have distinct biochemical properties from pRb, a separate physiological role for p107 has not yet been demonstrated.

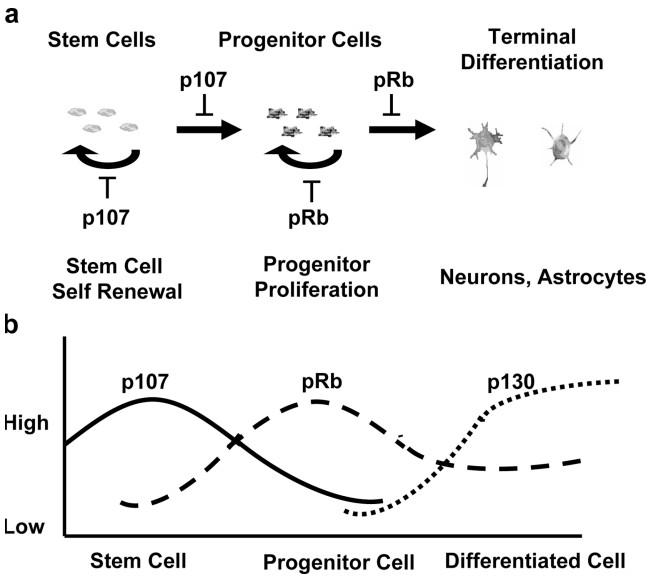

Figure 10. **p107 and pRb have distinct roles in neurogenesis.** (a) p107 negatively regulates the neural precursor cell pool by affecting both self-renewing and differentiative divisions. In contrast, pRb does not have an effect on the neural stem cell population but rather negatively regulates proliferation and differentiation of the neural progenitor population. (b) Temporal expression of Retinoblastoma family members. p107 expression is highest in the neural precursor population whereas pRB is expressed in dividing progenitor population and p130 is expressed in the differentiated population.

Our results show that p107, but not pRb, is responsible for the regulation of stem cell self-renewal. This distinct role for p107 in neural precursor regulation can be largely accounted for by the unique expression pattern of pRb and p107 in the brain. p107 is specifically expressed in uncommitted precursor cells and becomes rapidly down-regulated as cells commence differentiation (Callaghan et al., 1999). Our previous studies have shown that Rb is up-regulated and activated as cells initiate differentiation and is required for terminal mitosis after commitment to a neuronal fate (Slack et al., 1993, 1998; Jiang et al., 1997; Callaghan et al., 1999; Ferguson et al., 2000). Finally once differentiation is complete, p130 is up-regulated and believed to maintain cells in the differentiated state (Slack et al., 1993,1998; Jiang et al., 1997; Callaghan et al., 1999; Ferguson et al., 2000; Fig. 10 b). Hence, temporal regulation of the Retinoblastoma family proteins reveals that p107 is expressed in the uncommitted precursor pool and functions in a unique physiological role, which is to negatively regulate neural stem cell self-renewal (Fig. 10 a). This role for p107 in stem cell regulation may also explain its role in carcinogenesis, and why in some cases, both Rb and p107 must be absent for a tumor to develop (Maandag et al., 1994). For example in mice, neither Rb nor p107 mutations alone lead to retinal tumors, however, when p107 and pRb are both disrupted, retinoblastoma-like tumors develop (Maandag et al., 1994). Progenitor cells deficient in Rb will still have limited cycles

whereas the absence of p107 will further expand the stem cell pool and thereby enhance the input of progenitor cells to promote tumor formation.

In conclusion, our results reveal a unique role for p107 in neural precursor cell regulation whereby p107 controls the self-renewal capacity of neural stem cells. This is a novel niche for p107 that is attributable to its high expression in uncommitted neural precursor cells in the germinal zones. p107 may therefore represent a potential therapeutic target with which to expand the stem cell population in the adult brain.

Materials and methods

Mice

Germline p107-null mice were generated previously by LeCouter et al. (1998) and maintained on SV-129, Balb-C, and C57Bl/6 backgrounds. Germline Rb-null mice on a C57Bl/6 background strain, originally generated by Jacks et al. (1992) were obtained from Jackson ImmunoResearch Laboratories. To generate Rb/p107-deficient embryos, heterozygous ($Rb^{+/-}$) C57Bl/6 mice were crossed with $p107^{+/-}$ SV-129 mice to produce double heterozygous mice for $Rb^{+/-}$:$p107^{+/-}$. Double heterozygous mice were crossed to produce mice deficient for both Rb and p107 ($Rb^{-/-}$:$p107^{-/-}$), as well as $Rb^{-/-}$, $Rb^{+/-}$:$p107^{+/-}$, $p107^{-/-}$, and wild-type mice. Animals were genotyped according to standard protocols with primers published previously for p107 (LeCouter et al., 1998) and Rb (Jacks et al., 1992). For embryonic time points, the time of plug identification was counted as day 0.5. All experiments were approved by the University of Ottawa's Animal Care ethics committee adhering to the Guidelines of the Canadian Council on Animal Care.

Tissue fixation and cryoprotection

Pregnant female mice and adult mice were killed with a lethal injection of sodium pentobarbitol. Embryos were dissected and fixed overnight in 4% PFA in PBS, pH 7.4. Adult mice were perfused with PBS followed by cold 4% PFA and brains removed. Brains were then fixed overnight in 4% PFA, cryoprotected in 22% sucrose in PBS, frozen, and 14-μm coronal cryosections were collected on Superfrost Plus slides (12–550-15; Fisher Scientific).

BrdU labeling and immunohistochemistry

To assess neural progenitor and stem cell numbers in adult mice, intraperitoneal injections of BrdU (dissolved in 0.007 N/NaOH in 0.9% NaCl; 50 mg/kg^{-1} body mass) were given every 2 h over a 10-h period. Mice were killed 30 min (progenitor cells) or 4 wk (stem cells) after the last injection (Tropepe et al., 1997). BrdU detection was performed according to Ferguson et al. (2002). BrdU-positive cells were counted in the subependyma of the lateral ventricles in every 10th coronal cryosection (14 μm thick) from the most rostral crossing of the corpus callosum to the start of the 3rd ventricle (crossing of the anterior commissure). Student's *t* test was performed to compare the mean numbers of BrdU-positive cells and significant differences assessed at values of $\alpha = 0.05$.

Immunohistochemical staining was performed to detect BrdU-labeled cells with a mouse monoclonal anti-BrdU (1:100; 280879; Boehringer), neurons with anti-βIII tubulin (mouse monoclonal hybridoma supernatant, 1:50; Caccamo et al., 1989) or NeuN (1:200; MAB377; Chemicon), astrocytes with anti-GFAP (rabbit anti–bovine glial fibrillary acidic protein; 1:400; AB986; DakoCytomation), and oligodendrocytes with anti-O_4 (1:50; MAB345; Chemicon).

TUNEL staining

Apoptotic cells were detected in coronal sections of the lateral ventricles from adult wild-type ($n = 4$) and $p107^{-/-}$ ($n = 4$) brains using the TUNEL as described previously in Ferguson et al. (2002). TUNEL-positive cells were counted in the subependyma of the lateral ventricles in every 10th coronal cryosection (14-μm-thick) from the most rostral crossing of the corpus callosum to the start of the 3rd ventricle (crossing of the anterior commissure). Student's *t* test was performed to compare the mean numbers of TUNEL-positive cells and significant differences assessed at values of $\alpha = 0.05$.

Western blotting

Protein extracts were isolated from cultured neurospheres in lysis buffer, run on a 6% SDS-PAGE gel, and transferred to a nitrocellulose membrane as described in Ferguson et al. (2000). Immunoblotting was performed with antibodies directed against the cytoplasmic domain and full-length Notch1 (07–220; Upstate Biotechnology), p107 (sc-318; Santa Cruz Biotechnology Corp.), and actin (sc-1616; Santa Cruz Biotechnology Corp.). Blots were developed by chemiluminescence according to manufacturer's instructions (ECL; Amersham Biosciences).

Adenoviral expression of p107

To assess the effect of p107 levels on Notch1 expression, HEK 293 (human embryonic kidney) cells were infected with recombinant adenoviral vectors expressing GFP (control) or p107 and GFP. HEK 293 cells were plated in six-well Corning tissue culture dishes at a density of 5×10^4 cells/well and 24 h after plating cells were infected with three multiplicity of infection of recombinant adenoviral vectors expressing GFP (control) or p107 and GFP. 16 h after infection, cells were lysed and protein extracts were run on an SDS-PAGE for Western blot detection of Notch1, p107, and actin (loading control). The p107 vector was provided by Dr. S. Meloche (Universite de Montreal, Montreal, Canada) (Makris et al., 2002).

Neurosphere assay

Pregnant female mice were killed on gestation day 10 and the uterine horns removed and placed in HBSS. Embryos were removed from their amniotic sacs and their head primordia were dissected at the level of the first brachial arch according to the procedure of Tropepe et al. (1999). The epidermal ectoderm was removed and the telencephalic neuroepithelia dissected and transferred to a 1.5-ml Eppendorf tube containing 400 μl of serum-free stem cell media with 10 ng/ml^{-1} bFGF and 2 $\mu g/ml^{-1}$ heparin as described previously (Reynolds and Weiss, 1992; Tropepe et al., 1999). Neuroepithelia were mechanically dissociated and single cells were plated at a density of 10 cells/μl^{-1} in uncoated 24-well Nunclon plates (four to six wells per embryo, $n = 7$ wild type, 5 $Rb^{-/-}$, 6 $p107^{-/-}$, 6 $Rb^{-/-}$:$p107^{-/-}$, 8 $Rb^{+/-}$:$p107^{+/-}$). Primary neurospheres were counted 7 d after plating and Student's *t* tests were used to compare means with significant differences assessed at values of $\alpha = 0.05$.

To obtain neurospheres from adult mice, animals were killed, brains removed, and placed in artificial cerebrospinal fluid (aCSF). The lateral and medial walls of the lateral ventricles were dissected and then enzymatically and mechanically dissociated as described previously in Tropepe et al. (1997). Cells were plated as described above for embryonic tissue.

To assess whether the effect of p107 deletion on stem cell number was due to a cell autonomous or non-cell autonomous mechanism, we performed a dilution curve for the neurosphere assay. A fixed number of cells were plated at five different densities and the resulting total number of neurospheres were compared after 1 wk. If the number of neurospheres increased with increasing cell density one would interpret this as a non-cell autonomous effect whereas if there was no difference in the total number of neurospheres across the different dilutions one would interpret this as a cell autonomous effect. In this experiment, neurospheres from wild-type and $p107^{-/-}$ neurosphere cultures were mechanically dissociated to single cells and 10,000 cells were resuspended in increasing volumes of serum-free stem cell media so that final cell concentrations were 5, 2.5, 1.25, 0.625, and 0.3125 cells/μl^{-1}. Cells were plated in 200 μl volumes in 96-well plates and with increasing cell dilutions an increasing number of wells were plated to accommodate the 10,000 cells (Table II). 1 wk after plating, the total number of neurospheres were counted for each of the cell dilutions.

Table II. **Dilution curve for the neurosphere assay**

Cells plating density	Total volume for 10,000 cells	Number of cells/well	Number of wells
cells/μl	*ml*	*200 μl*	*10,000 cells*
5.0	2	1,000.0	10
2.5	4	500.0	20
1.25	8	250.0	40
0.625	16	125.0	80
0.3125	32	62.5	160

Initial plating densities in relation to the total volume for 10,000 cells at each density, the numbers of cells plated per 200 μl well, and total number of wells.

Self-renewal assay and assessment of multipotentiality

To assess neural stem cell self-renewal, individual primary neurospheres (7–8-d-old) of similar size (E10 ~200–250 μm, adults ~150–200 μm in diameter) were transferred to a fresh Eppendorf tube containing 200 μl of serum-free media and mechanically dissociated and transferred to individual wells in a 96-well plate (Tropepe et al., 1999). 7–8 d after plating, secondary neurospheres were counted per well (per primary neurosphere). To assess multipotentiality, 7–8-d-old secondary neurospheres were allowed to differentiate by plating on poly-L-ornithine–coated dishes in media containing 2% serum without FGF-2. A half media change was performed every 3 d and cultures were fixed with 4% PFA 10 d after plating for immunohistochemical analysis.

Assessment of progenitor cell regeneration after a [^{3}H]thymidine kill in adult mice

The [^{3}H]thymidine kill of neural progenitor cells was performed according to the protocol of Morshead et al. (1994). In brief, mice were given three injections of [^{3}H]thymidine with one injection every 4 h of 0.8 mCi injection^{-1} (specific activity 45–55 Ci/mmol^{-1}; ICN Biomedicals). 48 h after [^{3}H]thymidine injections, mice received five intraperitoneal injections of BrdU (50 mg/kg^{-1} body mass; one injection every 2 h) to label dividing cells. 30 min after the last injection, mice were killed, perfused with 4% PFA, and tissue was processed for BrdU immunohistochemistry. BrdU-positive cells were counted as described in the BrdU labeling and immunohistochemistry section.

In situ hybridization

Nonradioactive in situ hybridization and digoxigenin probe labeling was performed according to protocols described previously (Wallace and Raff, 1999). Antisense riboprobes for Notch1 (and sense), Delta-like 1, Hes1, and Hes5 were generated according to sequences published previously (Lindsell et al., 1995; Tomita et al., 1996; Gray et al., 1999). Sense and antisense riboprobes for p107 were provided by Drs. Z. Jiang and E. Zacksenhaus (University of Toronto, Toronto, Canada) (Jiang et al., 1997).

Chromatin immunoprecipitation

The Notch1 gene was analyzed for E2F consensus sequences with Genomatix promoter analysis software. Four sets of PCR primers were designed around four regions of E2F binding sequences, specifically, (a) the 2 E2F sites in intron 1, (b) the single E2F site in intron 2, (c) 2 E2F sites in 3′ region, and (d) the single E2F site in the 3′-untranslated region of the Notch1 gene (Fig. 4 b). Sequences for each set of PCR primers are as follows for intron 1, forward primer 5′AGTGAGGCGGAAGTGGACGGCA-3′, reverse primer 5′-CTGGAGATGCCTGCGAACAGG-3′, for intron 2, forward primer 5′-GCTTGTATCTTAGTATCTGTAT-3′ and reverse primer 5′-ACACAGTGACACTGCACCCCT-3′, for the 3′ region forward primer 5′-ACAGCATGCTCGAGCTGTCCA-3′ and reverse primer 5′-AGGAGGAGACTCCCCTGTTCCT-3′, and the 3′-untranslated region forward primer 5′-GGGGCAATTCTGGCCATGGCA-3′ and the reverse primer 5′-GTTTTTATACAAAATAAGAGGAC-3′.

Neurospheres were mechanically dissociated using fire-polished glass pipettes. Chromatin immunoprecipitations were performed according to manufacturer's instructions (Transduction Laboratories). A p107 antibody (Santa Cruz Biotechnologies) was used to immunoprecipitate p107–DNA complexes. Polymerase chain reaction was performed on the immunoprecipitated and control (input) DNA in four separate reactions for each of the primer sets above.

Microscopy

Sections treated for immunohistochemistry or in situ hybridization were examined by a Zeiss Axioskop 2 microscope with standard fluorescence and brightfield/darkfield settings at ×5 0.25 or ×20 0.50 NA objectives. Immunohistochemistry of cultured neurospheres were examined on a Zeiss Axiovert S100 microscope with standard fluorescence using an ×20 0.30 NA objective. Images were captured using a Sony Power HAD 3CCD color video camera with Northern Eclipse software. Figures were compiled using Adobe Photoshop 6.0. Manipulations of brightness and intensity were made equally to all treatment groups.

We are indebted to members of the Canadian Stem Cell Network, Drs. D. van der Kooy, C.M. Morshead, S. Weiss, V. Tropepe, and K.A. McClellan for their helpful discussions and critical review of this manuscript. We are also grateful to J. MacLaurin and W.C. McIntosh and S.M. Callaghan for their invaluable technical assistance and expertise.

This work was funded by grants from Canadian Institutes of Health Research (CIHR) and the Canadian Stroke Network (CSN) and Canadian Stem Cell Network to R.S. Slack. J.L. Vanderluit is a recipient of a CSN fellowship; K.L. Ferguson a CIHR studentship; V. Ruzhynsky an Ontario Graduate Scholarship studentship and S.M. McNamara a CSN summer studentship.

Submitted: 30 March 2004
Accepted: 3 August 2004

References

Beijersbergen, R.L., R.M. Kerkhoven, L. Zhu, L. Carlee, P.M. Voorhoeve, and R. Bernards. 1994. E2F-4, a new member of the E2F gene family, has oncogenic activity and associates with p107 in vivo. *Genes Dev.* 8:2680–2690.

Biebl, M., C.M. Cooper, J. Winkler, and H.G. Kuhn. 2000. Analysis of neurogenesis and programmed cell death reveals a self-renewing capacity in the adult rat brain. *Neurosci. Lett.* 291:17–20.

Caccamo, D., C.D. Katsetos, M.M. Herman, A. Frankfurter, V.P. Collins, and L.J. Rubinstein. 1989. Immunohistochemistry of a spontaneous murine ovarian teratoma with neuroepithelial differentiation. Neuron-associated beta-tubulin as a marker for primitive neuroepithelium. *Lab. Invest.* 60:390–398.

Callaghan, D.A., L. Dong, S.M. Callaghan, Y.X. Hou, L. Dagnino, and R.S. Slack. 1999. Neural precursor cells differentiating in the absence of Rb exhibit delayed terminal mitosis and deregulated E2F 1 and 3 activity. *Dev. Biol.* 207: 257–270.

Chen, H., A. Thiagalingam, H. Chopra, M.W. Borges, J.N. Feder, B.D. Nelkin, S.B. Baylin, and D.W. Ball. 1997. Conservation of the Drosophila lateral inhibition pathway in human lung cancer: a hairy-related protein (HES-1) directly represses achaete-scute homolog-1 expression. *Proc. Natl. Acad. Sci. USA.* 94:5355–5360.

Chiasson, B.J., V. Tropepe, C.M. Morshead, and D. van der Kooy. 1999. Adult mammalian forebrain ependymal and subependymal cells demonstrate proliferative potential, but only subependymal cells have neural stem cell characteristics. *J. Neurosci.* 19:4462–4471.

Clarke, A.R., E.R. Maandag, M. van Roon, N.M. van der Lugt, M. van der Valk, M.L. Hooper, A. Berns, and H. te Riele. 1992. Requirement for a functional Rb-1 gene in murine development. *Nature.* 359:328–330.

Cobrinik, D., M.H. Lee, G. Hannon, G. Mulligan, R.T. Bronson, N. Dyson, E. Harlow, D. Beach, R.A. Weinberg, and T. Jacks. 1996. Shared role of the pRB-related p130 and p107 proteins in limb development. *Genes Dev.* 10: 1633–1644.

Corotto, F.S., J.A. Henegar, and J.A. Maruniak. 1993. Neurogenesis persists in the subependymal layer of the adult mouse brain. *Neurosci. Lett.* 149:111–114.

Ewen, M.E., B. Faha, E. Harlow, and D.M. Livingston. 1992. Interaction of p107 with cyclin A independent of complex formation with viral oncoproteins. *Science.* 255:85–87.

Faha, B., M.E. Ewen, L.H. Tsai, D.M. Livingston, and E. Harlow. 1992. Interaction between human cyclin A and adenovirus E1A-associated p107 protein. *Science.* 255:87–90.

Ferguson, K.L., and R.S. Slack. 2001. The Rb pathway in neurogenesis. *Neuroreport.* 12:A55–A62.

Ferguson, K.L., S.M. Callaghan, O.H. MJ, D.S. Park, and R.S. Slack. 2000. The Rb-CDK4/6 signaling pathway is critical in neural precursor cell cycle regulation. *J Biol Chem.* 275:33593-600.

Ferguson, K.L., J.L. Vanderluit, J.M. Hebert, W.C. McIntosh, E. Tibbo, J.G. MacLaurin, D.S. Park, V.A. Wallace, M. Vooijs, S.K. McConnell, and R.S. Slack. 2002. Telencephalon-specific Rb knockouts reveal enhanced neurogenesis, survival and abnormal cortical development. *EMBO J.* 21:3337–3346.

Gill, R.M., R. Slack, M. Kiess, and P.A. Hamel. 1998. Regulation of expression and activity of distinct pRB, E2F, D-type cyclin, and CKI family members during terminal differentiation of P19 cells. *Exp. Cell Res.* 244:157–170.

Ginsberg, D., G. Vairo, T. Chittenden, Z.X. Xiao, G. Xu, K.L. Wydner, J.A. DeCaprio, J.B. Lawrence, and D.M. Livingston. 1994. E2F-4, a new member of the E2F transcription factor family, interacts with p107. *Genes Dev.* 8: 2665–2679.

Gray, G.E., R.S. Mann, E. Mitsiadis, D. Henrique, M.L. Carcangiu, A. Banks, J. Leiman, D. Ward, D. Ish-Horowitz, and S. Artavanis-Tsakonas. 1999. Human ligands of the Notch receptor. *Am. J. Pathol.* 154:785–794.

Hijmans, E.M., P.M. Voorhoeve, R.L. Beijersbergen, L.J. van't Veer, and R. Bernards. 1995. E2F-5, a new E2F family member that interacts with p130 in vivo. *Mol. Cell. Biol.* 15:3082–3089.

Hitoshi, S., T. Alexson, V. Tropepe, D. Donoviel, A.J. Elia, J.S. Nye, R.A. Conlon, T.W. Mak, A. Bernstein, and D. van der Kooy. 2002. Notch pathway molecules are essential for the maintenance, but not the generation, of mammalian neural stem cells. *Genes Dev.* 16:846–858.

Jacks, T., A. Fazeli, E.M. Schmitt, R.T. Bronson, M.A. Goodell, and R.A. Weinberg. 1992. Effects of an Rb mutation in the mouse. *Nature.* 359:295–300.

Jiang, Z., E. Zacksenhaus, B.L. Gallie, and R.A. Phillips. 1997. The retinoblastoma gene family is differentially expressed during embryogenesis. *Oncogene.* 14: 1789–1797.

LeCouter, J.E., B. Kablar, W.R. Hardy, C. Ying, L.A. Megeney, L.L. May, and M.A. Rudnicki. 1998. Strain-dependent myeloid hyperplasia, growth deficiency, and accelerated cell cycle in mice lacking the Rb-related p107 gene. *Mol. Cell. Biol.* 18:7455–7465.

Lee, E.Y., C.Y. Chang, N. Hu, Y.C. Wang, C.C. Lai, K. Herrup, W.H. Lee, and A. Bradley. 1992. Mice deficient for Rb are nonviable and show defects in neurogenesis and haematopoiesis. *Nature.* 359:288–294.

Lee, E.Y., N. Hu, S.S. Yuan, L.A. Cox, A. Bradley, W.H. Lee, and K. Herrup. 1994. Dual roles of the retinoblastoma protein in cell cycle regulation and neuron differentiation. *Genes Dev.* 8:2008–2021.

Lee, M.H., B.O. Williams, G. Mulligan, S. Mukai, R.T. Bronson, N. Dyson, E. Harlow, and T. Jacks. 1996. Targeted disruption of p107: functional overlap between p107 and Rb. *Genes Dev.* 10:1621–1632.

Lees, E., B. Faha, V. Dulic, S.I. Reed, and E. Harlow. 1992. Cyclin E/cdk2 and cyclin A/cdk2 kinases associate with p107 and E2F in a temporally distinct manner. *Genes Dev.* 6:1874–1885.

Levison, S.W., R.P. Rothstein, C.Y. Brazel, G.M. Young, and P.J. Albrecht. 2000. Selective apoptosis within the rat subependymal zone: a plausible mechanism for determining which lineages develop from neural stem cells. *Dev. Neurosci.* 22:106–115.

Li, Y., C. Graham, S. Lacy, A.M. Duncan, and P. Whyte. 1993. The adenovirus E1A-associated 130-kD protein is encoded by a member of the retinoblastoma gene family and physically interacts with cyclins A and E. *Genes Dev.* 7:2366–2377.

Lindsell, C.E., C.J. Shawber, J. Boulter, and G. Weinmaster. 1995. Jagged: a mammalian ligand that activates Notch1. *Cell.* 80:909–917.

Lindsten, T., J.A. Golden, W.X. Zong, J. Minarcik, M.H. Harris, C.B. Thompson, C.M. Cooper-Kuhn, M. Vroemen, J. Brown, H. Ye, et al. 2003. The proapoptotic activities of Bax and Bak limit the size of the neural stem cell pool. Impaired adult neurogenesis in mice lacking the transcription factor E2F1. *J. Neurosci.* 23:11112–11119.

Lipinski, M.M., and T. Jacks. 1999. The retinoblastoma gene family in differentiation and development. *Oncogene.* 18:7873–7882.

Lois, C., and A. Alvarez-Buylla. 1994. Long-distance neuronal migration in the adult mammalian brain. *Science.* 264:1145–1148.

Lois, C., J.M. Garcia-Verdugo, and A. Alvarez-Buylla. 1996. Chain migration of neuronal precursors. *Science.* 271:978–981.

Luskin, M.B. 1993. Restricted proliferation and migration of postnatally generated neurons derived from the forebrain subventricular zone. *Neuron.* 11:173–189.

Maandag, E.C., M. van der Valk, M. Vlaar, C. Feltkamp, J. O'Brien, M. van Roon, N. van der Lugt, A. Berns, and H. te Riele. 1994. Developmental rescue of an embryonic-lethal mutation in the retinoblastoma gene in chimeric mice. *EMBO J.* 13:4260–4268.

MacPherson, D., J. Sage, D. Crowley, A. Trumpp, R.T. Bronson, and T. Jacks. 2003. Conditional mutation of Rb causes cell cycle defects without apoptosis in the central nervous system. *Mol. Cell. Biol.* 23:1044–1053.

Makris, C., L. Voisin, E. Giasson, C. Tudan, D.R. Kaplan, and S. Meloche. 2002. The Rb-family protein p107 inhibits translation by a PDK1-dependent mechanism. *Oncogene.* 21:7891–7896.

Morrison, S.J., N.M. Shah, and D.J. Anderson. 1997. Regulatory mechanisms in stem cell biology. *Cell.* 88:287–298.

Morshead, C.M., C.G. Craig, and D. van der Kooy. 1998. In vivo clonal analyses reveal the properties of endogenous neural stem cell proliferation in the adult mammalian forebrain. *Development.* 125:2251–2261.

Morshead, C.M., B.A. Reynolds, C.G. Craig, M.W. McBurney, W.A. Staines, D. Morassutti, S. Weiss, and D. van der Kooy. 1994. Neural stem cells in the adult mammalian forebrain: a relatively quiescent subpopulation of subependymal cells. *Neuron.* 13:1071–1082.

Morshead, C.M., and D. van der Kooy. 1992. Postmitotic death is the fate of constitutively proliferating cells in the subependymal layer of the adult mouse brain. *J. Neurosci.* 12:249–256.

Nakamura, Y., S. Sakakibara, T. Miyata, M. Ogawa, T. Shimazaki, S. Weiss, R. Kageyama, and H. Okano. 2000. The bHLH gene hes1 as a repressor of the neuronal commitment of CNS stem cells. *J. Neurosci.* 20:283–293.

Ohtsuka, T., M. Sakamoto, F. Guillemot, and R. Kageyama. 2001. Roles of the basic helix-loop-helix genes Hes1 and Hes5 in expansion of neural stem cells of the developing brain. *J. Biol. Chem.* 276:30467–30474.

Potten, C.S., and M. Loeffler. 1990. Stem cells: attributes, cycles, spirals, pitfalls and uncertainties. Lessons for and from the crypt. *Development.* 110:1001–1020.

Reynolds, B.A., and S. Weiss. 1992. Generation of neurons and astrocytes from isolated cells of the adult mammalian central nervous system. *Science.* 255: 1707–1710.

Reynolds, B.A., and S. Weiss. 1996. Clonal and population analyses demonstrate that an EGF-responsive mammalian embryonic CNS precursor is a stem cell. *Dev. Biol.* 175:1–13.

Robey, E., D. Chang, A. Itano, D. Cado, H. Alexander, D. Lans, G. Weinmaster, and P. Salmon. 1996. An activated form of Notch influences the choice between CD4 and CD8 T cell lineages. *Cell.* 87:483–492.

Rossiter, J.P., R.J. Riopelle, and M.A. Bisby. 1996. Axotomy-induced apoptotic cell death of neonatal rat facial motoneurons: time course analysis and relation to NADPH-diaphorase activity. *Exp. Neurol.* 138:33–44.

Shingo, T., C. Gregg, E. Enwere, H. Fujikawa, R. Hassam, C. Geary, J.C. Cross, and S. Weiss. 2003. Pregnancy-stimulated neurogenesis in the adult female forebrain mediated by prolactin. *Science.* 299:117–120.

Slack, R.S., P.A. Hamel, T.S. Bladon, R.M. Gill, and M.W. McBurney. 1993. Regulated expression of the retinoblastoma gene in differentiating embryonal carcinoma cells. *Oncogene.* 8:1585–1591.

Slack, R.S., H. El-Bizri, J. Wong, D.J. Belliveau, and F.D. Miller. 1998. A critical temporal requirement for the retinoblastoma protein family during neuronal determination. *J. Cell Biol.* 140:1497–1509.

Stevaux, O., and N.J. Dyson. 2002. A revised picture of the E2F transcriptional network and RB function. *Curr. Opin. Cell Biol.* 14:684–691.

Tomita, K., M. Ishibashi, K. Nakahara, S.L. Ang, S. Nakanishi, F. Guillemot, and R. Kageyama. 1996. Mammalian hairy and Enhancer of split homolog 1 regulates differentiation of retinal neurons and is essential for eye morphogenesis. *Neuron.* 16:723–734.

Tropepe, V., C.G. Craig, C.M. Morshead, and D. van der Kooy. 1997. Transforming growth factor-alpha null and senescent mice show decreased neural progenitor cell proliferation in the forebrain subependyma. *J. Neurosci.* 17: 7850–7859.

Tropepe, V., M. Sibilia, B.G. Ciruna, J. Rossant, E.F. Wagner, and D. van der Kooy. 1999. Distinct neural stem cells proliferate in response to EGF and FGF in the developing mouse telencephalon. *Dev. Biol.* 208:166–188.

Vairo, G., D.M. Livingston, and D. Ginsberg. 1995. Functional interaction between E2F-4 and p130: evidence for distinct mechanisms underlying growth suppression by different retinoblastoma protein family members. *Genes Dev.* 9:869–881.

Wallace, V.A., and M.C. Raff. 1999. A role for Sonic hedgehog in axon-to-astrocyte signalling in the rodent optic nerve. *Development.* 126:2901–2909.

Wu, L., A. de Bruin, H.I. Saavedra, M. Starovic, A. Trimboli, Y. Yang, J. Opavska, P. Wilson, J.C. Thompson, M.C. Ostrowski, et al. 2003. Extra-embryonic function of Rb is essential for embryonic development and viability. *Nature.* 421:942–947.

Yoshikawa, K. 2000. Cell cycle regulators in neural stem cells and postmitotic neurons. *Neurosci. Res.* 37:1–14.